

# original report Role for Nucleotide Excision Repair Gene Variants in Oxaliplatin-Induced Peripheral Neuropathy

**Purpose** Oxaliplatin forms part of routine treatment of advanced colorectal cancer; however, it often causes severe peripheral neuropathy, resulting in treatment discontinuation. We sought to determine the molecular and cellular mechanism underlying this toxicity.

**Patients and Methods** We exome resequenced blood DNA samples from nine patients with advanced colorectal cancer who had severe peripheral neuropathy associated with oxaliplatin (PNAO) within 12 weeks of treatment. We Sanger sequenced the *ERCC4* and *ERCC6* open reading frames in 63 patients with PNAO and carried out targeted genotyping in 1,763 patients without PNAO. We tested the functionality of *ERCC4* variants using viability and DNA repair assays in *Schizosaccharomyces pombe* and human cell lines after exposure to oxaliplatin and ultraviolet light.

**Results** Exome resequencing identified one patient carrying a novel germline truncating mutation in the nucleotide excision repair (NER) gene *ERCC4*. This mutation was functionally associated with sensitivity to oxaliplatin ( $P = 3.5 \times 10^{-2}$ ). We subsequently found that multiple rare *ERCC4* nonsynonymous variants were over-represented in affected individuals ( $P = 7.7 \times 10^{-3}$ ) and three of these were defective in the repair of ultraviolet light-induced DNA damage ( $P < 1 \times 10^{-3}$ ). We validated a role for NER genes in PNAO by finding that multiple rare *ERCC6* nonsynonymous variants were similarly over-represented in affected individuals ( $P = 2.4 \times 10^{-8}$ ). Excluding private variants, 22.2% of patients (14 of 63 patients) with PNAO carried Pro379Ser or Glu875Gly in *ERCC4* or Asp425Ala, Gly446Asp, or Ser797Cys in *ERCC6*, compared with 8.7% of unaffected patients (152 of 1,750 patients; odds ratio, 3.0; 95% CI, 1.6 to 5.6;  $P = 2.5 \times 10^{-4}$ ).

**Conclusion** Our study provides evidence for a role of NER genes in PNAO, together with mechanistic insights.

JCO Precis Oncol. © 2018 by American Society of Clinical Oncology

Hannah West  
Michelle Coffey  
Michael J. Wagner  
Howard L. McLeod  
James P. Colley  
Richard A. Adams  
Oliver Fleck  
Timothy S. Maughan  
David Fisher  
Richard S. Kaplan  
Rebecca Harris  
Jeremy P. Cheadle

Author affiliations and support information (if applicable) appear at the end of this article.

None of the sponsors played a role in the study design or in the collection, analysis, and interpretation of the data.

**Corresponding author:** Jeremy P. Cheadle, PhD, Division of Cancer and Genetics, School of Medicine, Cardiff University, Heath Park, Cardiff, CF14 4XN, United Kingdom; e-mail: cheadlej@cardiff.ac.uk.

## INTRODUCTION

Oxaliplatin, a third-generation platinum drug, in combination with fluorouracil and leucovorin or oral capecitabine is standard treatment of locally advanced and metastatic colorectal cancer (CRC); it improves both response and progression-free survival.<sup>1,2</sup> It also improves disease-free survival in the adjuvant treatment of patients with stage II and III colon cancer.<sup>3</sup> In addition, oxaliplatin is widely used to treat other GI malignancies. Platinum agents exert their effects by forming inter- and intrastrand DNA cross-links,<sup>4</sup> which stall the cell cycle, inhibit DNA synthesis,<sup>5</sup> and trigger apoptosis.<sup>6</sup> Oxaliplatin also induces oxidative DNA damage.<sup>7</sup>

Peripheral neuropathy is a well-recognized dose-limiting toxicity of oxaliplatin.<sup>8,9</sup> High cumulative doses of oxaliplatin are associated with chronic peripheral nerve damage causing sensory ataxia and functional impairment.<sup>10</sup> Chronic sensory neuropathy has been observed in approximately half of patients who received oxaliplatin with infusional fluorouracil and leucovorin.<sup>11</sup> Importantly, it is neurotoxicity, rather than tumor progression, that is often the cause of treatment discontinuation.<sup>12</sup> Because neurotoxicity is not correlated with response,<sup>12</sup> it is considered a potentially avoidable adverse effect. The underlying cause of peripheral neuropathy is not known, although oxidative stress may be a contributing factor.<sup>13-15</sup>

Although numerous genetic associations with peripheral neuropathy have been proposed (*GSTP1*,<sup>16-19</sup> *AGXT*,<sup>20</sup> *ERCC1*,<sup>21,22</sup> *FARS2*,<sup>22</sup> *TAC1*,<sup>22</sup> *SCN10A*,<sup>23</sup> *SCN4A*,<sup>23</sup> *VAC14*,<sup>24</sup> and several genome-wide associated loci<sup>25,26</sup>), none have been independently validated and introduced into patient stratification. Here, we sought to delineate the underlying cause by exome resequencing patients with severe peripheral neuropathy after treatment with oxaliplatin-based chemotherapy.

## PATIENTS AND METHODS

### Patients

We analyzed blood DNA samples from unrelated patients with advanced CRC from the United Kingdom national COIN trial (ClinicalTrials.gov identifier: NCT00182715).<sup>27</sup> Patients were randomly assigned to receive continuous oxaliplatin and fluoropyrimidine chemotherapy, continuous chemotherapy plus cetuximab, or intermittent chemotherapy. In all patients, treatment was identical for the first 12 weeks apart from the choice of fluoropyrimidine and the random assignment to receive or not receive cetuximab. All patients gave fully informed consent for their samples to be used for bowel cancer research (approved by REC [04/MRE06/60]). We obtained the maximum grade of peripheral neuropathy after 12 weeks of treatment. Patients with grade 3 or 4 peripheral neuropathy or who had had an oxaliplatin dose reduction as a result of severe peripheral neuropathy were classified as suffering from peripheral neuropathy associated with oxaliplatin (PNAO). Patients with no or grade 1 peripheral neuropathy formed a control group and were classified as not having PNAO. Patients with grade 2 peripheral neuropathy were excluded to allow a better discrimination between the two patient groups.

### Molecular Analyses

We excluded known inherited neuropathies by carrying out multiplex ligation-dependent probe amplification analysis of *PMP22* (approximately 75% of patients with Charcot-Marie-Tooth syndrome, the most common form of inherited neuropathy, have a 1.4-MB duplication) and by examining the exome resequencing data for *PMP22* and 65 other genes associated with rare inherited neuropathies (Appendix).

Library fragments containing exomic DNA were collected using the Roche Nimblegen SeqCap EZ Exome Library (Roche, Basel, Switzerland) solution-based method. Massively parallel sequencing was performed on the Illumina Genome Analyzer (Illumina, San Diego, CA). On average, across the exome, we had 55% (range, 46% to 60%) coverage of the open reading frame (ORF) at 20-fold depth. FASTQ files were processed through a sequence analysis pipeline using Burrows-Wheeler Aligner software for sequence alignment and modules from the Broad Institute's Genome Analysis Toolkit (Cambridge, MA) to recalibrate quality scores, refine alignments around potential insertions or deletions (indels), eliminate duplicate reads, call indel and single nucleotide polymorphism (SNP) genotypes, generate quality control metrics, and apply quality filters to the genotype calls. SNP calls were annotated using ANNOVAR software. Polymerase chain reaction (PCR) and Sanger sequencing were carried out as described in the Appendix. *ERCC4* and *ERCC6* nonsynonymous variants were genotyped using KASPar (LGC, Teddington, United Kingdom) or BeadArray (Illumina) technologies (Appendix).

### Functional Analyses

Production of a *Schizosaccharomyces pombe rad16* base strain and the *rad16* wild-type vector, *Cre* recombinase-mediated cassette exchange, transformation of the base strain, site-directed mutagenesis, and treatment with oxaliplatin and ultraviolet light were carried out as described in the Appendix. Four hundred eighty Epstein-Barr virus-transformed human lymphoblastoid cell lines established from healthy white individuals (European Collection of Authenticated Cell Cultures, Salisbury, United Kingdom) were assayed for the *ERCC4* variants Pro379Ser, Arg576Thr, and Glu875Gly using KASPar. Three cell lines for each variant in a heterozygous state and wild-type controls (n = 3) were selected for the functional analyses. Cell lines were established in RPMI-1640 supplemented with 10% fetal bovine serum, penicillin and streptomycin, and -glutamine and maintained at 37°C and 5.0% carbon dioxide. Survival analyses were carried out as described in the Appendix. For DNA repair assays, cells were irradiated with 70 J of ultraviolet C, and aliquots were removed at 0, 4, 24, and 48 hours after treatment, sorted

by fluorescence-activated cell sorting for viable cells, and DNA extracted. DNA samples were probed for cyclobutane pyrimidine dimers (CPDs) using an enzyme-linked immunosorbent assay kit (Cell BioLabs, San Diego, CA), and absorbance was read at 450 nm using a plate reader, with a reference range of 620 nm (Appendix).

### Statistical and Bioinformatic Analyses

For association analyses, R v.3.3.2 ([www.r-project.org](http://www.r-project.org)) was used for the Pearson's  $\chi^2$  test or Fisher's exact test, where appropriate. Average survival data for oxaliplatin and ultraviolet light exposure in *S. pombe* were normalized to wild type and analyzed using SPSS v.23 (SPSS, Chicago, IL) analysis of variance (ANOVA) with Dunnett correction (after transformation using the arcsine function). For DNA repair assays, statistical analyses were performed in SPSS using a two-way ANOVA, with mutation status and treatment as the independent variables. The dependent variable was CPD quantification (in nanograms per milliliter) as a measure of DNA repair. Individual ANOVAs were run at 24 and 48 hours. In silico predictions for functional significance of nonsynonymous variants were determined using Align-Grantham Variation/Grantham Deviation. Linkage disequilibrium was obtained using Haploview v.4.2 (Broad Institute).

## RESULTS

Of the 2,445 patients with advanced CRC in the COIN trial, 23% of patients who received oxaliplatin and fluorouracil-based therapy and 16% of patients who received oxaliplatin and capecitabine-based therapy had severe (grade  $\geq 3$ ) peripheral neuropathy over the course of the trial.<sup>27</sup> We focused on patients with severe PNAO within the first 12 weeks of treatment (Appendix and Table 1) as a potentially enriched group for causal germline mutations (63 patients). Although fewer of these patients responded to treatment at 12 weeks (47%, 26 of 55 patients with response data; Table 1) compared with patients without PNAO (grade  $\leq 1$ ,  $n = 1,763$ ; 57%, 884 of 1,542 patients with response data), this was not statistically significant ( $P = 1.4 \times 10^{-1}$ ). Nine of the 63 patients with severe PNAO had exome resequencing of their germline blood

DNA samples. These patients were selected based on review of their medical notes and had no potentially confounding clinical complications. We identified, on average, 48 stop gains (range, 40 to 56 stop gains) and 88 indels (range, 73 to 111 indels) predicted to result in frameshift mutations, per patient exome (Appendix Table A1). We excluded known inherited neuropathies in these patients by *PMP22* dosage analysis and by examining the resequencing data for 66 candidate genes (no stop gains or truncating indels were predicted).

### Novel Truncating Mutation in *ERCC4*

Variants not present in dbSNP v.132 (assigned as novel; National Center for Biotechnology Information, Bethesda, MD) were considered most likely to cause PNAO; we identified on average eight novel stop gains (range, two to 11 stop gains) and 28 novel frameshifting indels (range, 16 to 57 indels) per patient (Appendix Table A1). We also considered that germline truncating mutations in genes involved in oxaliplatin transport, metabolism, or the repair of its associated damage might be responsible for PNAO; we identified 104 such genes from literature reviews (Appendix). All nine patients carried truncating variants in these selected genes (range, one to four variants); however, only one of these variants, in a single patient, was novel (Appendix Table A1). Patient 8 carried the novel stop gain Ser613X in the nucleotide excision repair (NER) gene *ERCC4*, which was confirmed by Sanger sequencing of an independent PCR product (Appendix Table A1). We did not find any other coding region variants in the second *ERCC4* allele in patient 8 after direct sequence analysis of the patient's entire ORF and flanking intronic sequences. Clinical review confirmed that this patient did not have xeroderma pigmentosum (XP; caused by biallelic *ERCC4* mutations).

We carried out a more comprehensive analysis of all known DNA repair genes (REPAIRtoire,  $n = 163$  genes, <http://repairtoire.genesilico.pl><sup>28</sup>; and, MD Anderson/Wood's Human DNA Repair List,  $n = 244$  genes, [www.mdanderson.org/documents/Labs/Wood-Laboratory/human-dna-repair-genes.html](http://www.mdanderson.org/documents/Labs/Wood-Laboratory/human-dna-repair-genes.html)<sup>29</sup>), including those in the base excision repair system that repair oxidative DNA damage,<sup>30</sup> but did not find any additional novel stop gains or truncating indels.



**Table 1.** Clinical Information and *ERCC4* and *ERCC6* Genotypes for 63 Patients With Severe PNAO (Continued)

Patient No.	Age (years)	Sex	Arm*	Chemotherapy	Response at 12 Weeks	Maximum Grade of PNAO at 12 Week	If Stopped, Stopped for Neurotoxicity Within 12 Weeks?	Random Assignment (days)	<i>ERCC4</i>		<i>ERCC6</i>													
									Pro379Ser	His466Gln	Arg576Thr	Ser613X	Glu875Gly	Asp425Ala	Gly466Asp	Pro694Leu	Ser797Cys	Gly929Arg	Phe1217Cys	Ala1296Thr	Phe1437Ile	Thr144Ile		
31	73	F	C	XELOX	Partial response	3	Y	64	n/n	n/n	n/n	n/n	n/n	n/n	n/n	n/n	n/n	n/n	n/n	n/n	n/n	n/n	n/n	
32†	75	M	A	OsMidG	Partial response	3	N	n/n	n/n	n/n	n/n	n/n	n/n	n/n	n/n	n/n	n/n	n/n	n/n	n/n	n/n	n/n	n/n	n/n
33	77	F	A	OsMidG	Stable disease	3	Y	76	n/n	n/n	n/n	n/n	n/n	n/n	n/n	n/n	n/n	n/n	n/n	n/n	n/n	n/n	n/n	n/n
34	73	F	B	OsMidG	Stable disease	3	Y	54	n/n	n/n	n/n	n/n	n/n	n/n	n/n	n/n	n/n	n/n	n/n	n/n	n/n	n/n	n/n	n/n
35‡	40	F	A	OsMidG	Progressive disease	3	Y	52	n/n	n/n	n/n	n/n	n/n	n/n	n/n	n/n	n/n	n/n	n/n	n/n	n/n	n/n	n/n	n/n
36	55	F	A	OsMidG	Stable disease	3	Y	79	n/n	n/n	n/n	n/n	n/n	n/n	n/n	n/n	n/n	n/n	n/n	n/n	n/n	n/n	n/n	n/n
37‡	69	F	A	XELOX	Partial response	3	N	n/n	n/n	n/n	n/n	n/n	n/n	n/n	n/n	n/n	n/n	n/n	n/n	n/n	n/n	n/n	n/n	n/n
38	78	M	B	XELOX	No assessment	3	N	n/n	n/n	n/n	n/n	n/n	n/n	n/n	n/n	n/n	n/n	n/n	n/n	n/n	n/n	n/n	n/n	n/n
39	67	M	C	XELOX	Partial response	3	N	n/n	n/n	n/n	n/n	n/n	n/n	n/n	n/n	n/n	n/n	n/n	n/n	n/n	n/n	n/n	n/n	n/n
40	65	M	B	OsMidG	No assessment	3	Y	78	n/n	n/n	n/n	n/n	n/n	n/n	n/n	n/n	n/n	n/n	n/n	n/n	n/n	n/n	n/n	n/n
41	69	M	B	XELOX	Stable disease	4	N	n/n	n/n	n/n	n/n	n/n	n/n	n/n	n/n	n/n	n/n	n/n	n/n	n/n	n/n	n/n	n/n	n/n
42‡	64	M	B	XELOX	Partial response	3	N	n/n	n/n	n/n	n/n	n/n	n/n	n/n	n/n	n/n	n/n	n/n	n/n	n/n	n/n	n/n	n/n	n/n
43	77	F	A	XELOX	Stable disease	3	Y	76	n/n	n/n	n/n	n/n	n/n	n/n	n/n	n/n	n/n	n/n	n/n	n/n	n/n	n/n	n/n	n/n
44‡	60	F	B	XELOX	Partial response	3	N	n/n	n/n	n/n	n/n	n/n	n/n	n/n	n/n	n/n	n/n	n/n	n/n	n/n	n/n	n/n	n/n	n/n
45‡	73	M	B	XELOX	Partial response	3	N	n/n	n/n	n/n	n/n	n/n	n/n	n/n	n/n	n/n	n/n	n/n	n/n	n/n	n/n	n/n	n/n	n/n
46	68	M	A	XELOX	Partial response	3	N	n/n	n/n	n/n	n/n	n/n	n/n	n/n	n/n	n/n	n/n	n/n	n/n	n/n	n/n	n/n	n/n	n/n
47‡	53	F	A	XELOX	Partial response	3	N	n/n	n/n	n/n	n/n	n/n	n/n	n/n	n/n	n/n	n/n	n/n	n/n	n/n	n/n	n/n	n/n	n/n
48	73	M	B	XELOX	Complete response	3	N	n/n	n/n	n/n	n/n	n/n	n/n	n/n	n/n	n/n	n/n	n/n	n/n	n/n	n/n	n/n	n/n	n/n
49‡	56	F	A	XELOX	Stable disease	3	N	n/n	n/n	n/n	n/n	n/n	n/n	n/n	n/n	n/n	n/n	n/n	n/n	n/n	n/n	n/n	n/n	n/n
50	40	F	C	XELOX	Partial response	3	Y	63	n/n	n/n	n/n	n/n	n/n	n/n	n/n	n/n	n/n	n/n	n/n	n/n	n/n	n/n	n/n	n/n
51‡	65	F	A	XELOX	Stable disease	3	N	n/n	n/n	n/n	n/n	n/n	n/n	n/n	n/n	n/n	n/n	n/n	n/n	n/n	n/n	n/n	n/n	n/n
52	67	F	B	XELOX	Stable disease	3	Y	48	n/n	n/n	n/n	n/n	n/n	n/n	n/n	n/n	n/n	n/n	n/n	n/n	n/n	n/n	n/n	n/n
53	73	M	B	XELOX	Stable disease	3	Y	70	n/n	n/n	n/n	n/n	n/n	n/n	n/n	n/n	n/n	n/n	n/n	n/n	n/n	n/n	n/n	n/n
54	74	F	C	XELOX	Partial response	3	N	n/n	n/n	n/n	n/n	n/n	n/n	n/n	n/n	n/n	n/n	n/n	n/n	n/n	n/n	n/n	n/n	n/n
55	63	F	B	XELOX	Partial response	3	Y	49	n/n	n/n	n/n	n/n	n/n	n/n	n/n	n/n	n/n	n/n	n/n	n/n	n/n	n/n	n/n	n/n
56	78	M	B	XELOX	Partial response	3	Y	67	n/n	n/n	n/n	n/n	n/n	n/n	n/n	n/n	n/n	n/n	n/n	n/n	n/n	n/n	n/n	n/n
57	62	F	A	OsMidG	Partial response	3	Y	68	n/n	n/n	n/n	n/n	n/n	n/n	n/n	n/n	n/n	n/n	n/n	n/n	n/n	n/n	n/n	n/n
58	61	M	A	XELOX	Stable disease	3	N	n/n	n/n	n/n	n/n	n/n	n/n	n/n	n/n	n/n	n/n	n/n	n/n	n/n	n/n	n/n	n/n	n/n
59	50	F	A	XELOX	Progressive disease	3	N	n/n	n/n	n/n	n/n	n/n	n/n	n/n	n/n	n/n	n/n	n/n	n/n	n/n	n/n	n/n	n/n	n/n
60	74	F	C	XELOX	Progressive disease	3	N	n/n	n/n	n/n	n/n	n/n	n/n	n/n	n/n	n/n	n/n	n/n	n/n	n/n	n/n	n/n	n/n	n/n

(Continued on following page)



### Functional Analysis of the *ERCC4* Stop Mutation

We investigated whether the *ERCC4* nonsense mutation induced sensitivity to oxaliplatin and ultraviolet light (which causes CPDs that are repaired by NER). We recreated the mutation in the *S. pombe* homolog *rad16* (Ser585X) in a base strain and a strain deficient in endonuclease *uve1* (an *S. pombe*-specific alternative ultraviolet light repair system). After oxaliplatin treatment, we observed decreased survival for *rad16-Ser585X* ( $P = 3.5 \times 10^{-2}$ ) in comparison with wild-type *rad16* (*rad16*<sup>+</sup>) and, in a similar range with a control *rad16*-deleted mutant (*rad16*Δ; Fig 1A). Similarly, we observed decreased survival of *uve1*Δ-*rad16-Ser585X* after treatment with ultraviolet light ( $P < 1 \times 10^{-3}$ ; Fig 1B).

### Multiple Rare *ERCC4* Variants Associated With Peripheral Neuropathy

We sought further evidence for a role of *ERCC4* in PNAO and Sanger sequenced the *ERCC4* ORF and flanking intronic sequences in all 63 patients with PNAO. We did not find any additional stop gains or truncating indels; however, we did identify four rare (minor allele frequencies < 5% in dbSNP) nonsynonymous variants

(Pro379Ser, rs1799802 in three patients; His466Gln, rs372950439 in one patient; Arg576Thr, rs1800068 in one patient; and Glu875Gly, rs1800124 in four patients; Table 1). Pro379Ser, Arg576Thr, and Glu875Gly were predicted to interfere with function (Table 2). We also identified one common nonsynonymous (Arg415Gln, rs1800067), three synonymous, and three 5' untranslated region (UTR) variants. We genotyped the *ERCC4* nonsynonymous variants in all COIN patients with available samples. His466Gln was not seen in any further patients. Each of the other rare variants was found more frequently in patients with PNAO compared with patients without PNAO (Table 2). Combined, significantly more patients with PNAO carried one of these variants (13.1%; eight of 61 patients) compared with patients without PNAO (5.2%; 87 of 1,671 patients;  $P = 7.7 \times 10^{-3}$ ).

The common variant Arg415Gln was found in similar proportions of patients with PNAO (14.3%; nine of 63 patients) and without PNAO (14.8%; 260 of 1,754 patients;  $P = 8.7 \times 10^{-1}$ ). An intronic variant in *ERCC4* (rs1799800) associated with late-onset bortezomib-associated neuropathy<sup>31</sup> was not associated with PNAO (found in 38.1% of patients with PNAO *v* 48.0% of patients without PNAO;  $P = 1.2 \times 10^{-1}$ ).

**Fig 1.** The *ERCC4* nonsense mutation induced sensitivity to oxaliplatin and ultraviolet (UV) light in a *Schizosaccharomyces pombe* (*rad16*) model system. Average percent survival from (A) four independent experiments after oxaliplatin treatment or (B) three independent experiments after treatment with UV light for a control *rad16* gene deletion mutant (*rad16*Δ) and *rad16-Ser585X* (mimics Ser613X seen in a patient with peripheral neuropathy associated with oxaliplatin), normalized to *rad16*<sup>+</sup>. For treatment with UV light, all strains were *uve1*Δ. Standard deviations are displayed as vertical bars.

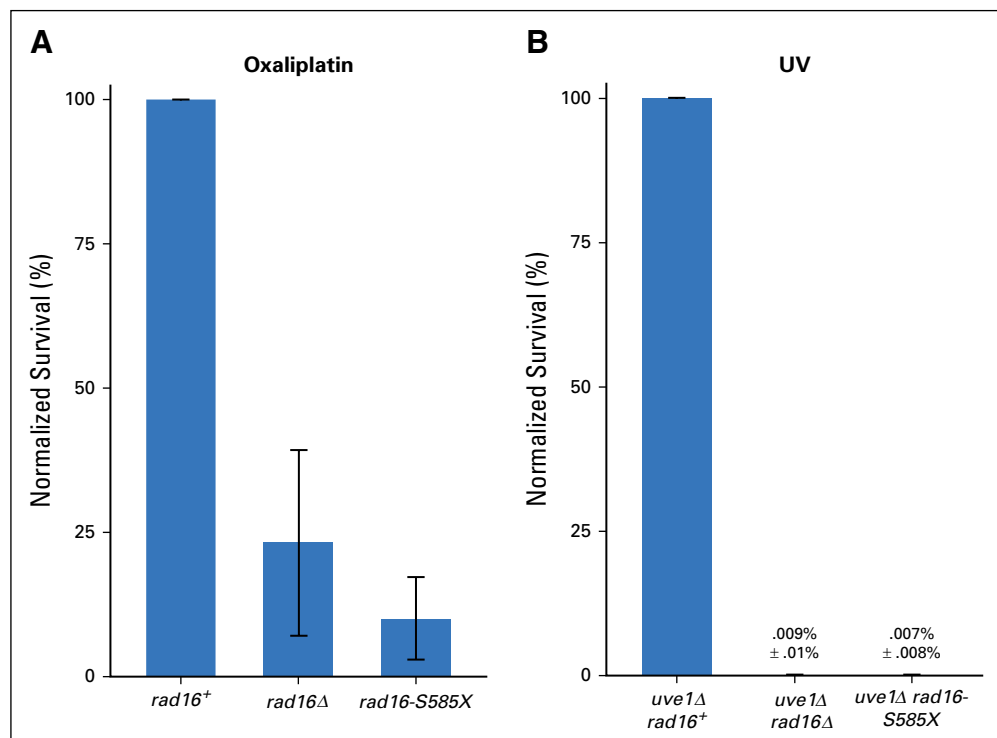


**Table 2.** Rare *ERCC4* Nonsynonymous and Stop-Gain Variants in Patients With and Without PNAO

Variant	rs No.	Align-GVGD Score*	No. of Patients/Total No. (%)		$\chi^2$	P
			With PNAO	Without PNAO		
Pro379Ser	rs1799802	C65	3/63 (4.8)	27/1,763 (1.5)	—	$8 \times 10^{-2}$
His466Gln	rs372950439	C15	1/61 (1.6)	0/1,677 (0)	—	—
Arg576Thr	rs1800068	C65	1/63 (1.6)	4/1,762 (0.2)	—	$1.6 \times 10^{-1}$
Ser613X	Novel	C65	1/63 (1.6)	—	—	—
Glu875Gly	rs1800124	C65	4/63 (6.4)	60/1,763 (3.4)	—	$2.8 \times 10^{-1}$
Total†			8/61 (13.1)	87/1,671 (5.2)	7.1	$7.7 \times 10^{-3}$
Excluding private variants			7/63 (11.1)	86/1,763 (4.9)	4.9	$2.7 \times 10^{-2}$

Abbreviations: Align-GVGD, Align-Grantham Variation/Grantham Deviation; PNAO, peripheral neuropathy associated with oxaliplatin; rs, reference single nucleotide polymorphism.

\*Score of predicted functional impact by Align-GVGD: C65 = most likely to affect function; and C15 = less likely to affect function.

†Ser613X was not included in the total because it was only assayed in patients with PNAO; one patient with PNAO carried Arg576Thr and Glu875Gly, and another without PNAO carried Pro379Ser and Glu875Gly. Values reflect the number of patients successfully genotyped (totals for all variants).

### Functional Analysis of *ERCC4* Nonsynonymous Variants

We sought evidence for causal effects of Pro379Ser, Arg576Thr, and Glu875Gly using Epstein-Barr virus-transformed human lymphoblastoid cell lines established from healthy individuals who carried each variant in a heterozygous state ( $n = 3$  for each variant and wild-type controls). Although treatment with ultraviolet light reduced viability in all lines, we did not observe any differences between wild-type and variant cell lines (data not shown). In terms of repair capacity after DNA damage with ultraviolet light, all wild-type cell lines showed noticeable repair 24 hours after treatment, with the majority of CPDs being repaired by 48 hours (Fig 2). In contrast, all three sets of variant cell lines displayed reduced repair in the initial ( $P < 1 \times 10^{-3}$  at both 24 and 48 hours) and validation ( $P < 1 \times 10^{-3}$  at both 24 and 48 hours) experiments (Fig 2).

### Validated Role for NER in PNAO

We attempted to validate a role for NER gene defects in PNAO and sought novel nonsynonymous variants in all *ERCC* gene family members by reanalyzing the exome resequencing data. We identified Gly929Arg in *ERCC6* in one patient, which was confirmed using an independent PCR product. We sought further potentially causal *ERCC6* variants by direct sequence analysis of the ORF, intronic boundaries, and 5'UTR in all 63 patients with PNAO. We identified nine

rare (Table 1) and five common nonsynonymous variants, two synonymous variants, and one 5'UTR variant; we genotyped nonsynonymous variants in all available patients. Seven rare nonsynonymous variants were predicted to be damaging (C55-C65), three of which (Asp425Ala, Pro694Leu, and Ser797Cys) were individually over-represented in patients with PNAO (Table 3). Combined, rare *ERCC6* nonsynonymous variants were highly associated with peripheral neuropathy (present in 20.6% of patients [13 of 63 patients] with PNAO *v* 4.7% of patients [82 of 1,749 patients] without PNAO;  $P = 2.4 \times 10^{-8}$ ; Table 3).

No common *ERCC6* nonsynonymous variants were associated with PNAO. In patients with PNAO *v* those without PNAO, Gly399Asp was found in 27.0% *v* 30.7% ( $P = 5.4 \times 10^{-1}$ ); Arg1213Gly was found in 36.5% *v* 34.6% ( $P = 7.6 \times 10^{-1}$ ); Arg1230Pro was found in 22.2% *v* 19.3% ( $P = 5.7 \times 10^{-1}$ ); and Gln1413Arg was found in 36.5% *v* 34.5%, respectively ( $P = 7.4 \times 10^{-1}$ ).

### Combined Analyses of *ERCC4* and *ERCC6*

Because private variants may skew statistical associations, we considered only rare *ERCC4* and *ERCC6* nonsynonymous variants that were present in two or more patients with PNAO. In total, 22.2% of patients with PNAO carried Pro379Ser or Glu875Gly in *ERCC4* or Asp425Ala, Gly446Asp, or Ser797Cys in *ERCC6*, compared with 8.7% of unaffected patients (odds ratio, 3.0; 95% CI, 1.6 to 5.6;  $P = 2.5 \times 10^{-4}$ ; Table 4).



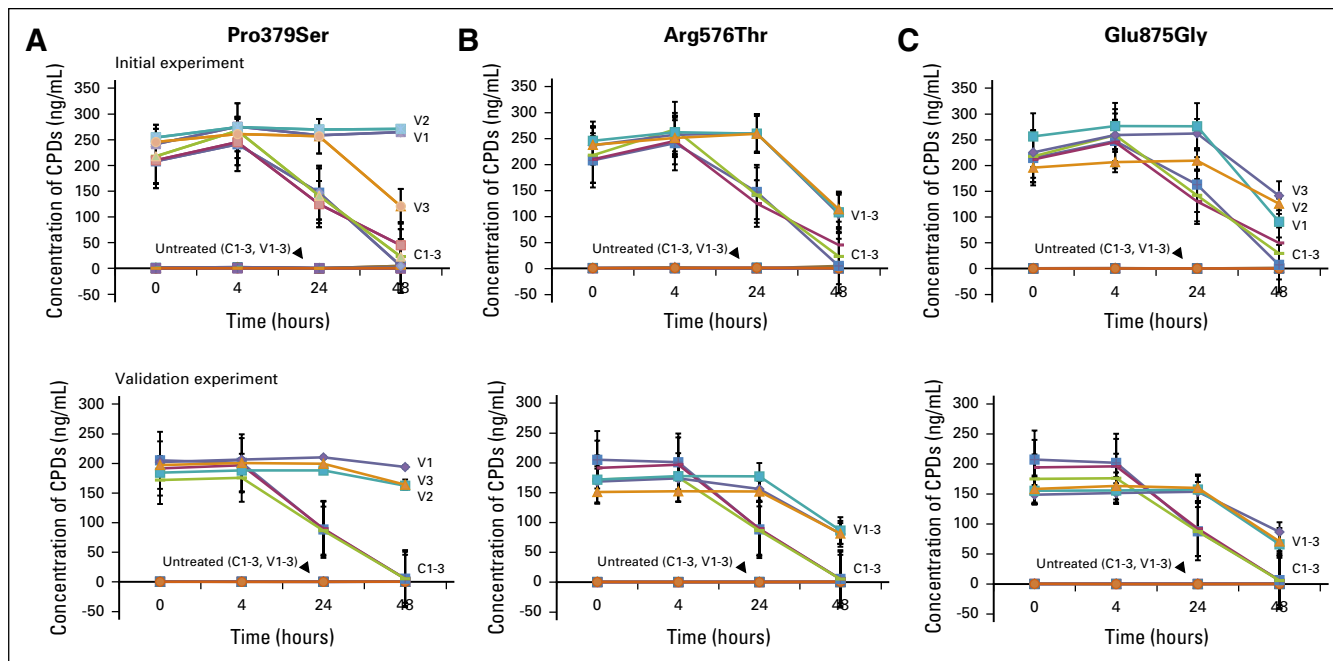


**Fig 2.** *ERCC4* nonsynonymous variants displayed reduced repair capacity. Average cyclobutane pyrimidine dimer (CPD) concentrations (in nanograms per milliliter) after ultraviolet C (70 J) irradiation in wild-type cells and cells carrying (A) Pro379Ser, (B) Arg576Thr, and (C) Glu875Gly over a 48-hour period, showing the initial (top panels) and validation (lower panels) experiments. CPD concentrations are plotted as an average of two duplicate samples from the same experiment run on separate enzyme-linked immunosorbent assay plates, which are shown against time with SE bars (data from the wild-type cells are shown in A, B, and C). The test and validation experiments were biologic repeats. 1-3, different cell lines; C, wild-type control cell line; V, variant cell line.

## DISCUSSION

The rare variant hypothesis predicts that individually rare but collectively common inherited variants play a significant role in disease susceptibility.<sup>32</sup> For example, rare nonsynonymous variants in the genes encoding apolipoprotein A1, the ATP binding cassette transporter A1 and lecithin cholesterol acyltransferase, are over-represented in individuals with low plasma levels of high-density lipoprotein cholesterol, a major risk factor for coronary atherosclerosis.<sup>33</sup> Furthermore, multiple rare nonsynonymous variants in *APC* play a significant role in inherited predisposition to colorectal adenomas.<sup>34</sup> Here, after identifying a novel *ERCC4* truncating mutation in a patient with PNAO, we found that multiple rare *ERCC4* and *ERCC6* nonsynonymous variants were over-represented in affected individuals. Therefore, the rare variant hypothesis may also be applicable to germline susceptibility to toxicity from therapy. If validated by others, the *ERCC4* and *ERCC6* nonsynonymous variants described herein would be considered moderately penetrant risk alleles for PNAO because a proportion of carriers did not have PNAO within 12 weeks of treatment.

*ERCC4* forms a complex with *ERCC1*, which carries out 5' incision of damaged DNA in NER, the main repair pathway involved in the removal of bulky and DNA-distorting adducts.<sup>35</sup>

The complex has also been implicated in inter-strand cross-link repair<sup>36</sup> and in the repair of double-strand breaks.<sup>37</sup> *ERCC6* encodes CSB, a SWI/SNF DNA-dependent related ATPase<sup>38</sup>; it is recruited to areas of DNA damage after stalling of RNA polymerase II and has multiple roles including chromatin remodeling<sup>39</sup> and recruitment of other NER proteins.<sup>40</sup> Given that *ERCC4* and *ERCC6* are likely targets of peripheral neuropathy-associated nonsynonymous variants, thorough examination of other NER genes is warranted to determine whether they play similar roles in toxicity to oxaliplatin.

Our finding that NER genes may play a role in oxaliplatin-induced peripheral neuropathy is supported by observations from several other studies. First, patients with *XPA*, *XPC*, *XPG*, and Cockayne syndrome-related disorders (caused by biallelic *ERCC* mutations) suffer from peripheral neuropathy before treatment.<sup>41</sup> The majority of our *ERCC4* or *ERCC6* carriers (17 of 20 patients) had only one locus-specific mutant allele, and to our knowledge, none had xeroderma pigmentosum or Cockayne syndrome group B, suggesting that haploinsufficiency for a mutant allele may be sufficient to induce peripheral neuropathy upon exposure to oxaliplatin. Second, an *Ercc1*<sup>-Δ</sup> murine model, which has reduced expression of the *ERCC4*-*ERCC1* complex, develops accelerated spontaneous peripheral neurodegeneration with significant structural alterations of the

**Table 3.** Rare *ERCC6* Nonsynonymous Variants in Patients With and Without PNAO

Variant	rs No.	Align-GVGD Score*	No. of Patients/Total No. (%)		$\chi^2$	P
			With PNAO	Without PNAO		
Asp425Ala	rs4253046	C65	3/63 (4.8)	15/1,763 (0.9)	—	$2 \times 10^{-2}$
Gly446Asp	rs4253047	C65	3/63 (4.8)	55/1,750 (3.1)	—	$4.5 \times 10^{-1}$
Pro694Leu	rs114852424	C65	1/63 (1.6)	0/1,763 (0)	—	$3 \times 10^{-2}$
Ser797Cys	rs146043988	C65	2/63 (3.2)	2/1,763 (0.1)	—	$1 \times 10^{-2}$
Gly929Arg	Novel	NA	1/63 (1.6)	1/1763 (0.1)	—	$7 \times 10^{-2}$
Phe1217Cys	rs61760166	C65	1/63 (1.6)	3/1,763 (0.2)	—	$1.3 \times 10^{-1}$
Ala1296Thr	rs139509516	C55	1/63 (1.6)	1/1,762 (0.1)	—	$7 \times 10^{-2}$
Phe1437Ile	rs758679804	C15	1/63 (1.6)	3/1,763 (0.2)	—	$1.3 \times 10^{-1}$
Thr1441Ile	rs4253230	C65	1/63 (1.6)	4/1,763 (0.2)	—	$1.6 \times 10^{-1}$
Total†			13/63 (20.6)	82/1,749 (4.7)	31.1	$2.4 \times 10^{-8}$
Excluding private variants			7/63 (11.1)	71/1,750 (4.1)	5.7	$1.7 \times 10^{-2}$

Abbreviations: Align-GVGD, Align-Grantham Variation/Grantham Deviation; NA, not applicable (alternative transcript); PNAO, peripheral neuropathy associated with oxaliplatin; rs, reference single nucleotide polymorphism.

\*Score of predicted functional impact: C65 = most likely to affect function; C55 = likely to affect function; and C15 = less likely to affect function.

†One patient with PNAO carried Asp425Ala and Ser797Cys, one patient without PNAO carried Asp425Ala and Gly446Asp, and another patient without PNAO carried Gly446Asp and Phe1217Cys. Values reflect the number of patients successfully genotyped (totals for all variants).

sciatic nerves.<sup>42</sup> Third, in *Xpa*<sup>-/-</sup> and *Xpc*<sup>-/-</sup> mice, chronic exposure to cisplatin resulted in an accelerated accumulation of unrepaired interstrand cross-links in neuronal cells.<sup>43</sup> Furthermore, the augmented adduct levels in dorsal root ganglion cells of these mice coincided with an earlier onset of peripheral neuropathy-like functional disturbance of their sensory nervous system.

Few predictive biomarkers for toxicity to therapy in the treatment of CRC have been independently validated. Two rare variants in *DPYD* have been associated with severe toxicity in patients receiving fluorouracil,<sup>44</sup> and a polymorphism

in *UGT-1A* has been linked to a higher risk of developing irinotecan-associated neutropenia and diarrhea<sup>45</sup>; however, none of these biomarkers have been introduced into routine clinical practice because of their poor sensitivity and specificity. Here, we identified roles for NER gene variants in toxicity to oxaliplatin, which, if validated, may represent an opportunity for patient stratification.

DOI: <https://doi.org/10.1200/PO.18.00090>

Published online on [ascopubs.org/journal/po](https://ascopubs.org/journal/po) on October 10, 2018.

**Table 4.** Combined Analysis of Nonprivate, Rare *ERCC4* and *ERCC6* Nonsynonymous Variants

Gene	Variants	No. of Patients/Total No. (%)		$\chi^2$	OR (95% CIs)	P
		With PNAO	Without PNAO			
<i>ERCC4</i>	Pro379Ser, Glu875Gly	7/63 (11.1)	86/1,763 (4.9)	4.9	—	$2.7 \times 10^{-2}$
<i>ERCC6</i>	Asp425Ala, Gly446Asp, Ser797Cys	7/63 (11.1)	71/1,750 (4.1)	5.7	—	$1.7 \times 10^{-2}$
Total*		14/63 (22.2)	152/1,750 (8.7)	13.4	3.0 (1.6 to 5.6)	$2.5 \times 10^{-4}$

Abbreviations: OR, odds ratio; PNAO, peripheral neuropathy associated with oxaliplatin.

\*Four patients without PNAO carried Glu875Gly in *ERCC4* and Gly446Asp in *ERCC6*, and another patient carried Pro379Ser in *ERCC4* and Gly446Asp in *ERCC6*.

## AUTHOR CONTRIBUTIONS

**Conception and design:** Howard L. McLeod, Richard A. Adams, Oliver Fleck, Timothy S. Maughan, Jeremy P. Cheadle

**Financial support:** Jeremy P. Cheadle

**Administrative support:** Howard L. McLeod, Richard A. Adams

**Provision of study material or patients:** Howard L. McLeod, Richard A. Adams, Timothy S. Maughan, Richard S. Kaplan, Jeremy P. Cheadle

**Collection and assembly of data:** Hannah West, Michelle Coffey, Michael J. Wagner, Howard L. McLeod, James P. Colley, Oliver Fleck, Timothy S. Maughan, David Fisher, Richard S. Kaplan, Rebecca Harris, Jeremy P. Cheadle

**Data analysis and interpretation:** Hannah West, Michelle Coffey, Michael J. Wagner, Howard L. McLeod, James P. Colley, Oliver Fleck, David Fisher, Jeremy P. Cheadle

**Manuscript writing:** All authors

**Final approval of manuscript:** All authors

**Accountable for all aspects of the work:** All authors

## AUTHORS' DISCLOSURES OF POTENTIAL CONFLICTS OF INTEREST

The following represents disclosure information provided by authors of this manuscript. All relationships are considered compensated. Relationships are self-held unless noted. I = Immediate Family Member, Inst = My Institution. Relationships may not relate to the subject matter of this manuscript. For more information about ASCO's conflict of interest policy, please refer to [www.asco.org/rwc](http://www.asco.org/rwc) or [ascopubs.org/po/author-center](http://ascopubs.org/po/author-center).

### Hannah West

No relationship to disclose

### Michelle Coffey

No relationship to disclose

### Michael J. Wagner

No relationship to disclose

### Howard L. McLeod

**Stock and Other Ownership Interests:** Cancer Genetics, Interpares Biomedicine

**Honoraria:** Genentech

**Consulting or Advisory Role:** Gentris, Cancer Genetics, Saladax Biomedical, National Institutes of Health/National Cancer Institute

### James P. Colley

No relationship to disclose

### Richard A. Adams

**Honoraria:** Merck Serono, SERVIER, Bristol-Myers Squibb, Amgen

**Consulting or Advisory Role:** Merck Serono, Amgen, SERVIER

**Speakers' Bureau:** Merck Serono

**Travel, Accommodations, Expenses:** SERVIER, Amgen, Merck Serono

### Oliver Fleck

No relationship to disclose

### Timothy S. Maughan

**Consulting or Advisory Role:** Vertex

### David Fisher

No relationship to disclose

### Richard S. Kaplan

**Honoraria:** Celldex

**Research Funding:** AstraZeneca (Inst)

### Rebecca Harris

No relationship to disclose

### Jeremy P. Cheadle

**Patents, Royalties, Other Intellectual Property:** Hold IPR and patents on MUTYH variants and have received royalties from Myriad

## ACKNOWLEDGMENT

We thank Simon Reed and Edgar Hartsuiker for helpful advice and Shelley Idziaszczyk, Rebecca Williams, Marc Naven, and Christopher Smith for technical support.

## Affiliations

Hannah West, Michelle Coffey, James P. Colley, Richard A. Adams, Rebecca Harris, and Jeremy P. Cheadle, School of Medicine, Cardiff University, Cardiff; Oliver Fleck, North West Cancer Research Institute, Bangor University, Bangor; Timothy S. Maughan, Cancer Research UK/Medical Research Council Oxford Institute for Radiation Oncology, University of Oxford, Oxford; David Fisher and Richard S. Kaplan, Medical Research Council Clinical Trials Unit, London, United Kingdom; Michael J. Wagner, Institute for Pharmacogenomics and Individualized Therapy, University of North Carolina, Chapel Hill, NC; and Howard L. McLeod, DeBartolo Family Personalized Medicine Institute, Moffitt Cancer Center, Tampa, FL.

## Support

Supported by Tenovus, the Kidani Trust, a Cancer Research UK development award from the Cardiff Cancer Research UK Centre, Cancer Research Wales, the Wales Gene Park, a Knowledge Economy Skills Scholarship, North West Cancer Research, and the Wales Assembly Government National Institute of Social Care and Health Research Cancer Genetics Biomedical Research Unit.

## REFERENCES

1. de Gramont A, Figuer A, Seymour M, et al: Leucovorin and fluorouracil with or without oxaliplatin as first-line treatment in advanced colorectal cancer. *J Clin Oncol* 18:2938-2947, 2000

2. Goldberg RM, Sargent DJ, Morton RF, et al: A randomized controlled trial of fluorouracil plus leucovorin, irinotecan, and oxaliplatin combinations in patients with previously untreated metastatic colorectal cancer. *J Clin Oncol* 22:23-30, 2004
3. André T, Boni C, Mounedji-Boudiaf L, et al: Oxaliplatin, fluorouracil, and leucovorin as adjuvant treatment for colon cancer. *N Engl J Med* 350:2343-2351, 2004
4. Brabec V, Kasparkova J: Modifications of DNA by platinum complexes: Relation to resistance of tumors to platinum antitumor drugs. *Drug Resist Updat* 8:131-146, 2005
5. Johnson NP, Hoeschele JD, Rahn RO, et al: Mutagenicity, cytotoxicity, and DNA binding of platinum(II)-chloroamines in Chinese hamster ovary cells. *Cancer Res* 40:1463-1468, 1980
6. Faivre S, Woynarowski JM: Oxaliplatin effects on DNA integrity and apoptosis induction in human tumor cells. *Proc Am Assoc Cancer Res* 39:158, 1998 (abstr 1081)
7. Afzal S, Jensen SA, Sørensen JB, et al: Oxidative damage to guanine nucleosides following combination chemotherapy with 5-fluorouracil and oxaliplatin. *Cancer Chemother Pharmacol* 69:301-307, 2012
8. Hartmann JT, Lipp HP: Toxicity of platinum compounds. *Expert Opin Pharmacother* 4:889-901, 2003
9. Weickhardt A, Wells K, Messersmith W: Oxaliplatin-induced neuropathy in colorectal cancer. *J Oncol* 2011:201593, 2011
10. Quasthoff S, Hartung HP: Chemotherapy-induced peripheral neuropathy. *J Neurol* 249:9-17, 2002
11. Krishnan AV, Goldstein D, Friedlander M, et al: Oxaliplatin-induced neurotoxicity and the development of neuropathy. *Muscle Nerve* 32:51-60, 2005
12. McWhinney SR, Goldberg RM, McLeod HL: Platinum neurotoxicity pharmacogenetics. *Mol Cancer Ther* 8:10-16, 2009
13. Di Cesare Mannelli L, Zanardelli M, Failli P, et al: Oxaliplatin-induced oxidative stress in nervous system-derived cellular models: Could it correlate with in vivo neuropathy? *Free Radic Biol Med* 61:143-150, 2013
14. Tabassum H, Waseem M, Parvez S, et al: Oxaliplatin-induced oxidative stress provokes toxicity in isolated rat liver mitochondria. *Arch Med Res* 46:597-603, 2015
15. Carozzi VA, Marmioli P, Cavaletti G: The role of oxidative stress and anti-oxidant treatment in platinum-induced peripheral neurotoxicity. *Curr Cancer Drug Targets* 10:670-682, 2010
16. Grothey A, McLeod HL, Green EM, et al: Glutathione S-transferase P1 I105V (GSTP1 I105V) polymorphism is associated with early onset of oxaliplatin-induced neurotoxicity. *J Clin Oncol* 23, 2005 (suppl; abstr 3509)
17. Ruzzo A, Graziano F, Loupakis F, et al: Pharmacogenetic profiling in patients with advanced colorectal cancer treated with first-line FOLFOX-4 chemotherapy. *J Clin Oncol* 25:1247-1254, 2007
18. Peng Z, Wang Q, Gao J, et al: Association between GSTP1 Ile105Val polymorphism and oxaliplatin-induced neuropathy: A systematic review and meta-analysis. *Cancer Chemother Pharmacol* 72:305-314, 2013
19. Lecomte T, Landi B, Beaune P, et al: Glutathione S-transferase P1 polymorphism (Ile105Val) predicts cumulative neuropathy in patients receiving oxaliplatin-based chemotherapy. *Clin Cancer Res* 12:3050-3056, 2006
20. Gamelin L, Capitain O, Morel A, et al: Predictive factors of oxaliplatin neurotoxicity: The involvement of the oxalate outcome pathway. *Clin Cancer Res* 13:6359-6368, 2007
21. Inada M, Sato M, Morita S, et al: Associations between oxaliplatin-induced peripheral neuropathy and polymorphisms of the ERCC1 and GSTP1 genes. *Int J Clin Pharmacol Ther* 48:729-734, 2010

22. Oguri T, Mitsuma A, Inada-Inoue M, et al: Genetic polymorphisms associated with oxaliplatin-induced peripheral neurotoxicity in Japanese patients with colorectal cancer. *Int J Clin Pharmacol Ther* 51:475-481, 2013
23. Argyriou AA, Cavaletti G, Antonacopoulou A, et al: Voltage-gated sodium channel polymorphisms play a pivotal role in the development of oxaliplatin-induced peripheral neurotoxicity: Results from a prospective multicenter study. *Cancer* 119:3570-3577, 2013
24. Hertz DL, Owzar K, Lessans S, et al: Pharmacogenetic discovery in CALGB (Alliance) 90401 and mechanistic validation of a VAC14 polymorphism that increases risk of docetaxel-induced neuropathy. *Clin Cancer Res* 22:4890-4900, 2016
25. Won HH, Lee J, Park JO, et al: Polymorphic markers associated with severe oxaliplatin-induced, chronic peripheral neuropathy in colon cancer patients. *Cancer* 118:2828-2836, 2012
26. Dolan ME, El Charif O, Wheeler HE, et al: Clinical and genome-wide analysis of cisplatin-induced peripheral neuropathy in survivors of adult-onset cancer. *Clin Cancer Res* 23:5757-5768, 2017
27. Maughan TS, Adams RA, Smith CG, et al: Addition of cetuximab to oxaliplatin-based first-line combination chemotherapy for treatment of advanced colorectal cancer: Results of the randomised phase 3 MRC COIN trial. *Lancet* 377:2103-2114, 2011
28. Milanowska K, Krwawicz J, Papaj G, et al: REPAIRtoire: A database of DNA repair pathways. *Nucleic Acids Res* 39:D788-D792, 2011
29. Wood RD, Mitchell M, Lindahl T: Human DNA repair genes, 2005. *Mutat Res* 577:275-283, 2005
30. Preston TJ, Henderson JT, McCallum GP, et al: Base excision repair of reactive oxygen species-initiated 7,8-dihydro-8-oxo-2'-deoxyguanosine inhibits the cytotoxicity of platinum anticancer drugs. *Mol Cancer Ther* 8:2015-2026, 2009
31. Broyl A, Corthals SL, Jongen JL, et al: Mechanisms of peripheral neuropathy associated with bortezomib and vincristine in patients with newly diagnosed multiple myeloma: A prospective analysis of data from the HOVON-65/GMMG-HD4 trial. *Lancet Oncol* 11:1057-1065, 2010
32. Fearnhead NS, Winney B, Bodmer WF: Rare variant hypothesis for multifactorial inheritance: Susceptibility to colorectal adenomas as a model. *Cell Cycle* 4:521-525, 2005
33. Cohen JC, Kiss RS, Pertsemlidis A, et al: Multiple rare alleles contribute to low plasma levels of HDL cholesterol. *Science* 305:869-872, 2004
34. Azzopardi D, Dallosso AR, Eliason K, et al: Multiple rare nonsynonymous variants in the adenomatous polyposis coli gene predispose to colorectal adenomas. *Cancer Res* 68:358-363, 2008
35. Reardon JT, Vaisman A, Chaney SG, et al: Efficient nucleotide excision repair of cisplatin, oxaliplatin, and bis-aceto-amine-dichloro-cyclohexylamine-platinum(IV) (JM216) platinum intrastrand DNA diadducts. *Cancer Res* 59:3968-3971, 1999
36. Kuraoka I, Kobertz WR, Ariza RR, et al: Repair of an interstrand DNA cross-link initiated by ERCC1-XPF repair/recombination nuclease. *J Biol Chem* 275:26632-26636, 2000
37. Ahmad A, Robinson AR, Duensing A, et al: ERCC1-XPF endonuclease facilitates DNA double-strand break repair. *Mol Cell Biol* 28:5082-5092, 2008
38. Troelstra C, van Gool A, de Wit J, et al: ERCC6, a member of a subfamily of putative helicases, is involved in Cockayne's syndrome and preferential repair of active genes. *Cell* 71:939-953, 1992
39. Citterio E, Van Den Boom V, Schnitzler G, et al: ATP-dependent chromatin remodeling by the Cockayne syndrome B DNA repair-transcription-coupling factor. *Mol Cell Biol* 20:7643-7653, 2000
40. Fousteri M, Vermeulen W, van Zeeland AA, et al: Cockayne syndrome A and B proteins differentially regulate recruitment of chromatin remodeling and repair factors to stalled RNA polymerase II in vivo. *Mol Cell* 23:471-482, 2006

41. Kanda T, Oda M, Yonezawa M, et al: Peripheral neuropathy in xeroderma pigmentosum. *Brain* 113:1025-1044, 1990
42. Goss JR, Stolz DB, Robinson AR, et al: Premature aging-related peripheral neuropathy in a mouse model of progeria. *Mech Ageing Dev* 132:437-442, 2011
43. Dzagnidze A, Katsarava Z, Makhlova J, et al: Repair capacity for platinum-DNA adducts determines the severity of cisplatin-induced peripheral neuropathy. *J Neurosci* 27:9451-9457, 2007
44. Schwab M, Zanger UM, Marx C, et al: Role of genetic and nongenetic factors for fluorouracil treatment-related severe toxicity: A prospective clinical trial by the German 5-FU Toxicity Study Group. *J Clin Oncol* 26:2131-2138, 2008
45. Hoskins JM, Goldberg RM, Qu P, et al: UGT1A1\*28 genotype and irinotecan-induced neutropenia: Dose matters. *J Natl Cancer Inst* 99:1290-1295, 2007

## Clinical Assessment

Clinical assessment of patients from the COIN trial occurred every 3 weeks, and toxicity data were recorded on clinical research forms at weeks 0, 6, 12, and 24. Toxicity was assessed using Common Terminology Criteria for Adverse Events version 3.0, in which peripheral sensory neuropathy was scored after consultation with a clinician and trials nurse. In addition, serious adverse event data were collected and reviewed by a centralized trials clinician. A quality-of-life questionnaire (European Organisation for Research and Treatment of Cancer Quality of Life Questionnaire C30) was also completed at 0, 6, 12, and 24 weeks. Patients with severe peripheral neuropathy had a minimum of grade 3 toxicity within the first 12 weeks of treatment, which was backed up by quality-of-life data.

## Molecular Analyses and Exome Resequencing

Using the exome resequencing data, the following genes associated with rare inherited neuropathies were analyzed: *PMP22*, *AARS*, *AIFM1*, *ATL1*, *ATP7A*, *BICD2*, *BSCL2*, *CCT5*, *CTDP1*, *DCTN1*, *DHTKD1*, *DNAJB2*, *DNM2*, *DNMT1*, *DYNC1H1*, *EGR2*, *FAM134B*, *FBLN5*, *FGD4*, *GARS*, *GDAP1*, *GJB1*, *GNB4*, *HARS*, *HINT1*, *HK1*, *HSPB1*, *HSPB3*, *HSPB8*, *IGHMBP2*, *IKBKAP*, *KARS*, *KIF1A*, *KIF5A*, *LITAF*, *LMNA*, *LRSAM1*, *MARS*, *MED25*, *MFN2*, *MPZ*, *MTMR13*, *MTMR2*, *MYH14*, *NDRG1*, *NGFB*, *NTRK1*, *PDK3*, *PLEKHG5*, *PRNP*, *PRPS1*, *PRX*, *RAB7*, *REEP1*, *SBF1*, *SCN9A*, *SETX*, *SH3TC2*, *SLC5A7*, *SPTLC1*, *SPTLC2*, *TFG*, *TRIM2*, *TRPV4*, *WNK1*, and *YARS*.

Genes potentially involved in the pharmacokinetics and mechanism of action of platinum compounds were identified from literature reviews. Four genes were involved in drug influx (*OCT1*, *OCT2*, *CTRI*, and *bMATE1*), three in trafficking (*CCS*, *COX17*, and *SOD1*), seven in detoxification (*MT1A*, *MT2A*, *NQO1*, *GSTT1*, *GSTP1*, *GSTM1*, and *MPO*), two in oxalate metabolism (*AGXT* and *GRHPR*), three in sequestration (*ATP7A*, *ATP7B*, and *HAH1*), 32 in DNA damage response and subsequent signaling pathways (*SPT16*, *SSRP1*, *HMGGB1*, *RAG1*, *RAG2*, *ABL1*, *RBI*, *p53*, *p73*, *AURKA*, *CCNG2*, *p38MAPK*, *MSK1*, *MKK3*, *MKK6*, *Histone H3*, *ERK*, *MEK1*, *MEK2*, *JNK*, *MKK4*, *MKK7*, *MPK1*, *AKT*, *NF- $\kappa$ B*, *XIAP*, *Bax*, *APAF1*, *CYC*, *CASP3*, *CASP6*, and *CASP9*), 46 in DNA damage repair and the associated response pathways (*POLB*, *POLH*, *POLM*, *REV3L*, *FANCA*, *FANCB*, *FANCC*, *FANCD2*, *FANCE*, *FANCF*, *FANCG*, *FANCI*, *FANCL*, *FANCM*, *FANCN*, *FAAP100*, *RM1*, *FAN1*, *MLH1*, *MSH2*, *MSH6*, *PMS2*, *ATM*, *ATR*, *CHEK1*, *CHEK2*, *BRCA1*, *BRCA2*, *GADD45*, *DDB2*, *CDC25C*, *CDC2*, *CSA*, *HR23B*, *RNApolIII*, *RP41*, *ERCC1*, *ERCC2*, *ERCC3*, *ERCC4*, *ERCC5*, *ERCC6*, *XPA*, *XRCC1*, *XRCC3*, and *MGMT*), and seven in drug efflux (*ABCC1*, *ABCC2*, *ABCC3*, *ABCC4*, *ABCC5*, *ABCB1*, and *ABCG2*).

## Polymerase Chain Reaction and Sanger Sequencing

Thermal cycling conditions consisted of an initial denaturation at 94°C for 10 minutes, followed by 32 cycles of 94°C for 30 seconds, 57°C for 30 seconds, and 72°C for 30 seconds, followed by a final elongation stage of 72°C for 10 minutes. Polymerase chain reaction (PCR) products were purified using ExoSap, in which 15  $\mu$ L of PCR product was incubated with 2 U of exonuclease I (New England Biolabs, Ipswich, MA) and 2 U of shrimp alkaline phosphatase (GE Healthcare, Chicago, IL). The reaction mixture was incubated at 37°C for 1 hour, followed by denaturation at 80°C for 15 minutes. After purification, PCR products were sequenced using the BigDye v3.1 Sequencing kit (Applied Biosystems, Foster City, CA). Thermal cycling parameters consisted of 24 cycles of 94°C for 10 second, 50°C for 5 seconds, and 60°C for 3 minutes and 30 seconds. Purification of sequencing products was carried out using an isopropanol-based method. Samples were run on an ABI 3100 genetic analyzer (Applied Biosystems), and sequence data were viewed using Sequencher v4.6 (Gene Codes, Ann Arbor, MI).

## Single Nucleotide Polymorphism Genotyping

Genotyping of Arg415Gln (rs1800067) in *ERCC4* and Gly399Asp (rs2228528), Arg1213Gly (rs2228527), and Gln1413Arg (rs2228529) in *ERCC6* was carried out using Illumina's Fast-Track Genotyping Service using their high-throughput BeadArray technology (Illumina, San Diego, CA). The overall genotyping success rate was 99.9% (8,731 of 8,744 genotypes were called successfully), and the concordance rate for previously sequenced samples ( $n = 63$ ) was 100% (252 of 252 genotypes were concordant). Genotyping of Pro379Ser (rs1799802), Arg576Thr (rs1800068), His466Gln (rs372950439), Glu875Gly (rs1800124), and rs1799800 in *ERCC4* and of Asp425Ala (rs4253046), Gly446Asp (rs4253047), Pro694Leu (rs114852424), Ser797Cys (rs146043988), Gly929Arg (novel), Phe1217Cys (rs61760166), Arg1230Pro (rs4253211), Ala1296Thr (rs139509516), Thr1441Ile (rs4253230), and Phe1437Ile (rs758679804) in *ERCC6* was carried out by LGC (Teddington, United Kingdom) using KASPar technology. The overall genotyping success rate was 97.5% (33,415 of 34,320 genotypes were called successfully), and the concordance rate for previously sequenced samples ( $n = 63$ ) was 99.9% (881 of 882 genotypes were concordant). We did not genotype the *ERCC6* variant Met1097Val because it was in high linkage disequilibrium with Arg1213Gly and Gln1413Arg (Met1097Val-Arg1213Gly;  $r^2 = 1.0$ ,  $D' = 1.0$ ; Met1097Val-Gln1413Arg;  $r^2 = 1.0$ ,  $D' = 1.0$ ; Arg1213Gly-Gln1413Arg;  $r^2 = 0.99$ ,  $D' = 1.0$ ). We Sanger sequenced samples that failed genotyping, that were outliers of cluster plots, or that carried variants to validate genotype calls.

## Functional Studies in *Schizosaccharomyces pombe*

### Construction of *S. pombe rad16* base strain.

The creation of a base strain for *rad16* was achieved using primers containing 100 nucleotides of sequence immediately upstream and downstream of *rad16*. In addition, these primers carried sequences corresponding to regions upstream and downstream of *ura4* in the plasmid pAW1 (shown in lowercase; forward: 5'-TCCATCCAAATTGGAAAATTTTCGCATCAAAGTATTTAACAGCTTTCAGAAATCAAATTTGCAAATTTGGAAAATCTCTACGAATAACACCACCATTAAATcggatccccgggtaattaa-3'; reverse: 5'-TTATTAATTAGGTGCGCTTAACATTCATATATATGGTGAACCAATATATATCAGATGTAGAAGCAAAAATTAATATATACAAAATTTATAAAAAAATAAAgaattcggagctcgtttaaac-3'). Amplification of *ura4* in pAW1 (linearized with *AccI*; New England Biolabs) was achieved by PCR to produce a 2.1-kb product consisting of *ura4* flanked by *loxP/loxM* sites (*loxP-ura4-loxM*) and *rad16* gene sequences, as previously described (Watson AT, et al: Gene 407:63-74, 2008). Transformation of this PCR product into *S. pombe* was carried out using the lithium acetate method. Transformants were grown on minimal medium lacking uracil and restreaked on plates containing the same medium. A replica plate was irradiated with 150 J/m<sup>2</sup> of ultraviolet light to identify those with ultraviolet sensitivity, a characteristic of *rad16* loss. Transformants with significantly decreased survival were selected and checked by colony PCR. Extracted DNA was sequenced at 5' and 3' *lox* sites to ensure their integrity.

### *rad16* wild-type PCR product with flanking *lox* sites.

The creation of a *rad16* wild-type PCR product with flanking *lox* sites (*loxP-rad16-loxM3*) was performed using primers designed with *lox* sites incorporated (forward: 5'-GGGATAACTTCGTATAGCATACATATACGAAGTTATATGCATCATCATCATCATGGAGGAGGAGAAACAAAGGTTCAATTTGCC-3'; reverse: 5'-GGGATAACTTCGTATATAATACATATACGAAGTTATTTACTCATAGTCCTTTAACTGTTTTTCGG-3'). PCR on *S. pombe* DNA was carried out using Phusion polymerase (New England Biolabs), with thermal cycling conditions consisting of an initial denaturation of 98°C for 2 minutes, followed by 30 cycles of 98°C for 30 seconds, 47°C for 30 seconds, and 72°C for 3 minutes and 30 seconds, with a final elongation of 72°C for 10 minutes. PCR products were cleaned using a NucleoSpin Gel and PCR Clean-Up kit (Macherey-Nagel, Bethlehem, PA).

### *Cre* recombinase-mediated cassette exchange.

*Cre* recombinase-mediated cassette exchange was carried out using a pAW8-*ccdB* plasmid and the *loxP-rad16-loxM3* PCR product; 170 ng of pAW8-*ccdB*, 90 ng of *loxP-rad16-loxM3* PCR product, and 2 U of *Cre* recombinase (New England Biolabs) were incubated at 37°C for 30 minutes, followed by 70°C for 10 minutes. One microliter of the *Cre* reaction product was transformed into 25  $\mu$ L of DH5 $\alpha$  electrocompetent cells and incubated at 30°C on LB plus ampicillin plates for 48 hours. Growth of colonies indicated that the toxic *ccdB* gene had successfully been replaced with *rad16* at the *lox* sites in pAW8. After plasmid mini-preparations, restriction digest with *Bam*HI (New England Biolabs) confirmed the insertion of *rad16*. The *rad16* open reading frame was sequenced from a number of transformants to ensure its integrity.

### Transformation of pAW8-*rad16* into base *S. pombe* strain.

The wild-type pAW8-*rad16* plasmid was transformed into the *S. pombe rad16* base strain using the lithium acetate method. Cells were incubated for 4 days on Edinburgh minimal medium plates with added thiamine and without leucine. Successful colonies were restreaked on master plates of the same composition for 2 days. After this point, colonies were selected and propagated in YEL (liquid complex medium) to facilitate loss of the plasmid and to eliminate further *Cre* recombinase action. Aliquots of the cultures were plated on YEA plates with added 5-fluoroorotic acid (1 g/L) to allow for growth of *ura4*<sup>-</sup> cells, which were streaked on master plates. Ultraviolet light treatment was used to distinguish colonies with restored nucleotide excision repair function. Colony PCR was performed to confirm that *rad16* had replaced *ura4*. Upon confirmation, a selection of transformants was sequenced to determine the integrity of the *lox* sites and the surrounding sequence. Functionality of the strains transformed with the wild-type *rad16* was performed to determine any potential detrimental effects associated with the incorporation of the *lox* sites flanking the *rad16* region. This was done by treatment with 100 J/m<sup>2</sup> of ultraviolet light. The wild-type *rad16* with flanking *lox* sites showed similar survival to unaltered wild-type *S. pombe* strains.



### Site-directed mutagenesis.

Site-directed mutagenesis was carried out using a Quikchange II XL Site-Directed Mutagenesis Kit (Agilent, Santa Clara, CA). Primers were designed with the sequence for Ser585X incorporated (forward: 5'-GTACTATGGAGGATaGATTGAG-GAGCAAAA-3'; reverse: 5'-TTTTTGCTCCTCAATCtATCCTCCATAGTAC-3'). Following the manufacturer's protocol, mutant strand synthesis was achieved by the addition of primers to 10 ng of pAW8-*rad16*. Thermocycling conditions consisted of an initial denaturation at 95°C for 1 minute, followed by 18 cycles of 95°C for 50 seconds, 60°C for 50 seconds, and 68°C for 6 minutes, and a final elongation at 68°C for 7 minutes. Digestion of the methylated paternal strands was achieved by addition of 10 U of *DpnI* and incubation at 37°C for 1 hour. XL10-Gold cells were transformed with 2 µL of the *DpnI*-treated plasmid, and 250 µL of cells were plated out on LB plus ampicillin plates. Plates were incubated at 37°C for 16 hours, and inserts of plasmids from transformants were sequenced to ensure that mutagenesis had been successful. The *S. pombe rad16* base strain was subsequently transformed with pAW8-*rad16-Ser585X*, and transformants with the truncating mutation were identified by colony PCR and sequencing.

### Construction of *uve1Δ* strains.

OL2112 (*b<sup>+</sup> uve1::LEU2 leu1-32 ura4-D18*) was crossed with the *rad16Δ* base strain (*smt-0 rad16::loxP-ura4-loxM leu1-32 ura4-D18*). Strains were mixed on sporulation medium (malt extract agar), incubated for 2 days at 30°C, and treated for 30 minutes with 30% ethanol to kill vegetative cells. Spores were plated on MMA, and colonies were genotyped. The resulting strain was named OL2116 (*b<sup>+</sup> rad16::loxP-ura4-loxM uve1::LEU2 leu1-32 ura4-D18*). Next, *uve1Δ* was combined with *loxP-rad16-loxM* and *loxP-rad16-S585X-loxM*. The resulting strains were OL2123 (*smt-0 loxP-rad16-loxM uve1::LEU2 leu1-32 ura4-D18*) and OL2131 (*smt-0 loxP-rad16-S585X-loxM uve1::LEU2 leu1-32 ura4-D18*).

### Drug and ultraviolet light treatments.

A primary culture of cells was grown overnight in YEL with shaking at 30°C; 10<sup>7</sup> cells were cultured in YEL with and without 1 mM of oxaliplatin. For the untreated cultures, an equivalent volume of dimethyl sulfoxide was added. Cells were incubated for 18 hours with shaking at 30°C, subsequently diluted to a range of concentrations, and plated on YEA plates in duplicate. For ultraviolet light treatment, appropriate numbers of cells were irradiated with ultraviolet light using a Stratalinker (Agilent; 5 J/m<sup>2</sup> for OL2116 [*rad16Δ uve1Δ*] and OL2131 [*rad16-S585X uve1Δ*] and 20 J/m<sup>2</sup> for OL2112 [*uve1Δ*]). Plates were incubated at 30°C for 4 days, and survival rates were determined by counting colonies of treated compared with untreated plates.

## Functional Studies in Human Cells

### Survival analyses.

Before survival analyses, 3 × 10<sup>6</sup> cells/mL were serum starved for 1 hour before treatment with ultraviolet light (40 Jm<sup>-2</sup>s<sup>-1</sup>) irradiation. Cell viability was measured by Trypan blue exclusion during a 48-hour period. Data were normalized to the initial viability at 0 hours and analyzed using analysis of variance.

### DNA repair assays.

Cells were centrifuged at 1,200 rpm for 5 minutes and resuspended in serum free media. Cells were irradiated with 70 J of ultraviolet C in large single-well dishes using an ultraviolet light crosslinker. Cells were resuspended in normal tissue culture media containing fetal bovine serum and antibiotics, and aliquots were removed at 0, 4, 24, and 48 hours after treatment for analysis. Aliquots of cells were sorted by fluorescence-activated cell sorting, and viable cells were retrieved (purity > 98%) before DNA extraction. DNA samples were probed for cyclobutane pyrimidine dimers (CPDs) using an enzyme-linked immunosorbent assay (ELISA) kit according to the manufacturer's instructions (Cell BioLabs, San Diego, CA). Briefly, DNA samples and a DNA standard conjugated to a known amount of CPDs were converted to single-stranded DNA by incubation at 96°C for 10 minutes followed by rapid chilling on ice for 10 minutes. DNA was diluted to 200 ng/mL in cold phosphate-buffered saline and incubated overnight at 4°C before ELISA. Wells were washed twice with cold phosphate-buffered saline, followed by hour-long incubations at room temperature with assay diluent, primary CPD antibody, blocking reagent, and secondary horseradish peroxidase-conjugated antibody, with wash steps between each incubation. Substrate solution was added to each well and incubated for 20 minutes at room temperature, before the addition of stop solution. Duplicate DNA samples from wild-type and variant cell lines were assayed on separate ELISA plates, and readings were averaged. This data were then validated by reassaying further duplicate DNA samples from independent experiments. Absorbance was read at 450 nm using a plate reader, with a reference range of 620 nm.

**Table A1.** Truncating Variants Identified Within the Whole Exome or the Oxaliplatin Transport, Metabolism, or DNA Repair Pathways

Type of Variant and Level of Analysis	Patient No. (No. of truncating variants)								
	1	2	3	4	5	6	7	8	9
Stop gain									
Whole exome									
Total	43	51	46	40	56	52	51	48	45
Novel	2	10	6	7	10	10	11	8	6
Oxaliplatin transport, metabolism, or DNA repair pathways									
Total	1	1	1	2	1	1	1	2	1
Novel	0	0	0	0	0	0	0	1 <i>ERCC4</i> Ser613X	0
Truncating indel									
Whole exome									
Total	73	111	80	86	85	99	91	77	93
Novel	16	57	21	20	16	41	28	18	39
Oxaliplatin transport, metabolism, or DNA repair pathways									
Total	2	1	1	1	1	0	3	0	0
Novel	0	0	0	0	0	0	0	0	0

NOTE. Numbers of variants are shown, together with the sole novel truncating variant, Ser613X in *ERCC4*. Variants not present in dbSNP v.132 (assigned as novel) were considered most likely to cause peripheral neuropathy associated with oxaliplatin.